



The role of T2-weighted images in assessing the grade of extraprostatic extension of the prostate carcinoma

Aslihan Onay¹ · Gokhan Ertas² · Metin Vural³ · Evrim Colak⁴ · Tarik Esen⁵ · Baris Bakir⁶

© Springer Science+Business Media, LLC, part of Springer Nature 2020

Abstract

Purpose Extraprostatic extension (EPE) is an unfavorable prognostic factor and the grade of EPE is also shown to be correlated with the prognosis of prostate cancer. The current study assessed the value of prostate magnetic resonance imaging (MRI) in measuring the radial distance (RD) of EPE and the role of T2 WI signs in predicting the grade of EPE.

Materials and methods A total of 110 patients who underwent prostate MRI before radical prostatectomy are enrolled in this retrospective study. Eighty-four patients have organ confined disease and the remaining twenty-six patients have EPE all verified by histopathology. Prostate MRI examinations were conducted with 3T MRI scanner and phased array coil with the following sequences: T2 WI, T1 WI, DCE, DWI with ADC mapping, and high *b*-value at $b = 1500 \text{ s/mm}^2$. The likelihood of EPE with 5-point Likert scale was assigned, several MRI features were extracted for each dominant tumor identified by using T2 WI. Tumors with Likert scales 4–5 were evaluated further to obtain MRI-based RD. The relationship between pathological and MRI-determined RD was tested. Univariate and multivariate logistic regression models were developed to detect the grade of pathological EPE. The inputs were among the 2 clinical parameters and 4 MRI features.

Results There is a moderate correlation between pathological RD and MRI-determined RD ($\rho = 0.45$, $P < 0.01$). In univariate and multivariate models, MRI features and clinical parameters possess varying significance levels (univariate models; $P = 0.048$ – 0.788 , multivariate models; $P = 0.173$ – 0.769). Multivariate models perform better than the univariate models by offering fair to good performances (AUC = 0.69 – 0.85). The multivariate model that employs the MRI features offers better performance than the model employs clinical parameters (AUC = 0.81 versus 0.69).

Conclusion Co-existence of T2 WI signs provide higher diagnostic value even than clinical parameters in predicting the grade of EPE. Combined use of clinical parameters and MRI features deliver slightly superior performance than MRI features alone.

Keywords Prostate cancer · Extraprostatic extension · Grade · MR imaging · Logistic regression

✉ Aslihan Onay
aslionay@gmail.com

Gokhan Ertas
gokhan.ertas@yeditepe.edu.tr

Metin Vural
metinvural@gmail.com

Evrin Colak
ecolak@ankara.edu.tr

Tarik Esen
tesen@ku.edu.tr

Baris Bakir
drbarisbakir@yahoo.com

² Department of Biomedical Engineering, Yeditepe University, 34755 Kayisdagi, Istanbul, Turkey

³ Department of Radiology, VKV American Hospital, 34365 Sisli, Istanbul, Turkey

⁴ Department of Electrical and Electronics Engineering, Ankara University, Bahcelievler Mah, 06830 Golbasi, Ankara, Turkey

⁵ Department of Urology, School of Medicine, Koc University, Davutpasa Street No:4, Topkapi, 34010 Istanbul, Turkey

⁶ Department of Radiology, Istanbul Faculty of Medicine, Istanbul University, Capa, Fatih, 34093 Istanbul, Turkey

¹ Department of Radiology, School of Medicine, Baskent University, Maresal Fevzi Cakmak Blvd, No: 45, Cankaya, Ankara, Turkey

Introduction

Presence of extraprostatic extension (EPE) in prostate cancer promotes higher tumor recurrence after radical prostatectomy (RP) and worse prognosis when compared to organ confined disease [1]. Additionally, clinical outcomes of the tumors with EPE show variations depending on the grade of EPE [2–5]. In quantification and sub-classification of EPE from pathologic specimens, there exist three different methods accepted commonly [3–6]. EPE has been subdivided into focal versus non-focal categories where focal EPE is defined as a few neoplastic glands beyond the prostate in only one or two slides [3]. A more objective approach suggests to discriminate focal EPE from non-focal EPE where focal EPE is present in less than one high-power field on no more than two separate sections [4]. Another method relies on measuring the radial distance (RD) of EPE. The radial distance of EPE is defined as the perpendicular distance of the prostate tumor extension that protrudes beyond the outer margin of the prostatic stroma [5]. Recent studies show that this measure may also act as an independent prognostic indicator for biochemical recurrence (BCR) risk after RP [6–8]. There is no correlation for continuous values of RD though a correlation is present when a threshold for RD is considered [7, 8]. However, there is no consensus for the optimal threshold value though the median value of the RD is reported to demonstrate correlation at a certain degree.

In predicting pathologic EPE non-invasively, use of prostate magnetic resonance images (MRI) has been reported to be valuable [9–11] and improved predications are attainable when MRI features are evaluated jointly with the clinical risk measures [12–15]. MRI features including the presence/absence of capsular bulge and irregularity (CBI), presence/absence of overt EPE (OEPE), presence/absence of neurovascular infiltration (NVI), presence/absence of obliteration of rectoprostatic angle (ORA) are based on subjective visual assessment of these features on T2 WI and shown to be linked with EPE diagnosis [17]. On the other hand, for discrimination of low-grade (focal) EPE from and high-grade (non-focal) EPE, there are no unified criteria for these MRI features though there are some efforts [16]. This study aims to find out the value of T2 WI sequence in measuring the RD of extraprostatic extension of prostate carcinoma and to investigate the value of subjective T2 WI signs in assessing the grade of EPE.

Materials and methods

Patient population and MR imaging

This retrospective study received approval from the local ethics and research committee. We included the patients with pathologically proven prostate cancer who had mp-MRI prior to RP procedure. Patients with long time interval (> 6 months) between Mp-MRI and RP, short time interval (< 6 weeks) between prostate biopsy and Mp-MRI and patients with prior hormonal or radiation treatment for prostate cancer were excluded from the study. Search on the electronic databases at our institution for the years between 2012 and 2017 revealed 2129 patients having biopsy proven prostate cancer and prostate MRI. However, among these patients, 121 patients underwent RP but only 110 of them satisfied the inclusion criteria completely and were enrolled in the current study, consequently.

Prostate MRI was performed on a 3T MR scanner (Magnetom Skyra, Siemens Medical Solutions, Erlangen, Germany) equipped with a sixteen-channel phased array surface coil. 20 mg of butylscopolamine (Buscopan, Boehringer) was intramuscularly injected to the patient prior to imaging to avoid artifacts due to bowel peristalsis during imaging. The imaging protocol consisted of T2 WI in axial, sagittal and coronal plane, axial diffusion-weighted imaging (DWI), and axial fat-suppressed dynamic contrast-enhanced imaging (DCE) with dedicated repetition time (TR), echo time (TE), field of view (FOV), and slice thickness (ST). For T2 WI, TR/TE = 3566–3631/100 ms; matrix size = 512 × 352; FOV = 200 mm; ST = 3 mm. For DWI, TR/TE = 4000/101 ms; matrix size = 192 × 154; FOV = 260 × 260 mm; ST = 3.6 mm with 0.3 mm slice gap; $b = 0, 50, 100, 200, 400, 600, \text{ and } 800 \text{ s/mm}^2$; number of excitations = 9 with apparent diffusion coefficient (ADC) mapping. For DCE imaging, TR/TE = 4.86/1.76 ms; matrix size = 192 × 154; FOV = 260 × 260 mm; ST = 3.6 mm.

Pathological analysis and assessment of pathological measures

All prostate specimens were fixed in 10% buffered neutral formalin and surgical margins were painted with ink. From apex to base, the step sectioning of entire prostate gland including seminal vesicles was acquired at intervals of 3–4 mm in the plane perpendicular to long axis of prostate gland. The sections were stained with hematoxylin and eosin. An experienced genitourinary pathologist marked an index lesion regarding to the following criteria: a prostate tumor showing EPE to outer margin of prostatic

stroma was considered as the index lesion. If none of the tumor foci had EPE, the tumor foci with the highest ISUP grading score were assumed as the index lesion. If the tumor foci have the same ISUP grading score, the maximum tumor size determined the index lesion.

For an index lesion identified, the uropathologist recorded the ISUP grading score, the presence or absence of EPE, the presence or absence of seminal vesicle invasion (SVI), and status of surgical margins. In the presence of EPE, the length of tumor protrusion perpendicular to the outer margin of the prostatic stroma, was measured by using an ocular micrometer and assigned as the pathologic RD. In the presence of multiple foci of EPE, the focus with maximum extension from the RP specimens was taken into account, while pathologic RD was considered to be zero in the absence of EPE [18]. Median value of the non-zero pathologic RDs obtained for the study dataset was used as the cut-off value to distinguish high-grade EPE from low-grade EPE.

MR image evaluation and assessment of MR measures

Two genitourinary radiologists with 12 and 5 years of experience in genitourinary radiology (*, and *) evaluated all the images produced during prostate MRI by mutual agreement. The radiologists knew that all the patients had histopathologically proven prostate tumor but they were blinded to the final pathology results regarding to the location of tumor foci and the status of extraprostatic disease. The radiologists identified the dominant tumor showing the lowest signal intensity on T2-WI and/or the lowest signal intensity on ADC maps from DWI and assessed seven MRI features for the tumor on T2-WI as follows:

- (1) Presence or absence of CBI (i.e., regional capsular spiculation and/or intraprostatic dominant tumor with smooth, convex bulging into extraprostatic space),
- (2) Presence or absence of OEPE (i.e., gross extension of prostate tumor into the periprostatic space),
- (3) Presence or absence of ORA (i.e., loss of the fatty space between rectum and prostate gland),
- (4) Presence or absence of NAI (i.e., unequal appearance of neurovascular bundle due to ipsilateral infiltration with prostate tumor),
- (5) Presence or absence of seminal vesicle invasion (i.e., loss of the high signal within the seminal vesicles).
- (6) Radial distance (i.e., MRI-determined RD). The distance was measured for a lesion with positive EPE assessed by a 5-point Likert scale. The 5-point Likert scale of EPE was evaluated by using the modified PI-RADS criteria of ESUR [10]: 1 = EPE absent (Normal tissue can be visualized between intact prostate capsule and tumor), 2 = EPE probably not present (Tumor abuts prostate capsule), 3 = Equivocal for EPE (Tumor abuts and causes irregularity on prostate capsule), 4 = EPE probably present (Tumor bulges, deforms, and obscures the prostate capsule), 5 = EPE absolutely present (Gross and measurable tumor is identified). Accordingly, any scale of 1, 2, or 3 lesion was assumed as negative for EPE, while any scale 4 or 5 lesion was presumed as positive for EPE. The RD was the maximum distance of the lesion that protruded beyond the outer margin of prostate being perpendicular to outer margin of prostate on the images (see Fig. 1a, b).

An index lesion was matched with histopathological diagram as reference standard with consensus of the uropathologist and radiologist by taking into account of alterations on the shape and size of the prostate caused by preservation of

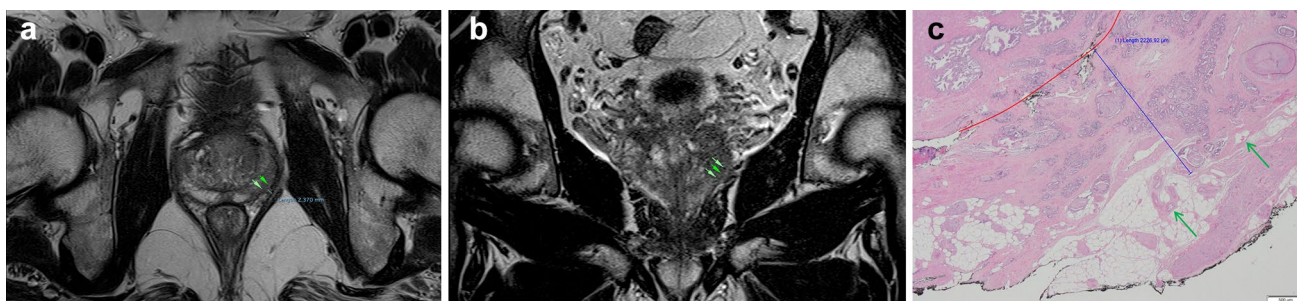


Fig. 1 a–c A 62-year-old man with 4+3 Gleason Score tumor in left posteromedial peripheral zone with histologically verified EPE. **a, b** Axial and coronal T2-weighted images demonstrating a prostate lesion that bulges the prostate capsule and cause capsular loss and having Likert scale of 4 (arrows). The maximum diameter of the bulging prostate tumor was measured as MRI-determined radial distance from axial T2 WI. Radial distance of prostate tumor (green

arrow) has been obtained by measuring the maximum distance that the tumor bulged beyond the prostate capsule (red line) radially from whole mount step section of the radical prostatectomy **c** pathologic radial distance of the tumor is 1 mm and its length is 2 mm (3DHISTECH Panoramic Desk II—Slide Scanner device, $\times 20$ objective)

specimens. The subjective EPE assessment was examined by using the RP specimens as the reference.

Logistic regression analysis

Numerous logistic regression models were designed to predict EPE and the grade of EPE. The inputs of these models were among the two clinical parameters namely the logarithm of the prostate-specific antigen (PSA) and D'Amico risk stratification (DRS) for the prostate cancer, and among the four MRI-determined measures CBI, OEPE, NAI, and ORA assessed by the radiologists. A number of models performing univariate logistic regression analysis were developed to determine the detection performances of each clinical parameter and each MRI-determined measure. Various models performing multivariate logistic regression analysis were developed to unveil the benefits of combined use of the clinical parameters or/and the MRI measures.

Statistical analysis

The relationship between pathologic RD and the corresponding MRI-determined RD was assessed using Spearman–rho correlation. In detection of EPE and discrimination of high-grade EPE from low-grade EPE, sensitivity (Se), specificity (Sp), positive predictive value (PPV), and negative predictive value (NPV) were calculated. Logistic regression analyses incorporating clinical parameters and/or MRI-determined measures were performed by randomly sampling participants with replacements and by using 1000 bootstrap samples, and reported by 95% confidence intervals considering the 2.5th and 97.5th percentiles of the bootstrap resampling distribution. The *t*-statistics were used to assess the relative importance of the parameters in the logistic regression models. Detection performance of each model

was determined by obtaining the receiving operating characteristic (ROC) curve and by computing the area under the curve (AUC). The performance was considered excellent, good, fair, poor, and fail if AUC was 0.90–1.00, 0.80–0.89, 0.70–0.79, 0.60–0.69, and 0.50–0.59, respectively. *P* value of < 0.05 was considered for statistical significance. The Se, Sp, PPV, and NPV were also calculated for detection of seminal vesicle invasion. All analyses, statistics and computations were performed using IBM SPSS for Windows (v25; Armonk, NY).

Results

Table 1 shows the demographic and clinical data of the 110 patients enrolled in the current study. The mean time interval between the prostate MRI and the RP procedure is 73.1 days (range 11–192 days). Eighty-four patients have EPE negative prostate lesion (i.e., organ confined disease) and the remaining 26 patients have lesions with EPE positive, all verified by histopathology. Five patients have seminal vesicle invasion based on RP specimens. Six of 110 patients show positive surgical margin. Positive surgical margin is only identified in six patients. Among these, five patients have EPE and the rest patient has organ confined disease. The median pathologic RD calculated for the EPE positive lesions is 1.0 mm (range 0.2–7.0 mm; mean: 1.6 mm).

All dominant lesions suspected on MRI are matched with the index lesion in the RP specimens. On the other hand, three of the dominant lesions studied are undetectable on mp-MRI images, however, these lesions are all EPE negative. In prediction of EPE from MRI, the 5-point Likert scoring shows low sensitivity but very high specificity leading to low positive and high negative predictive values (Se = 0.52, Sp = 0.90, PPV = 0.63, and NPV = 0.86). In

Table 1 Demographical and clinical characteristics of the patients

	Organ confined disease	EPE	
		Low grade	High grade
Number of patients	84	15	11
Age (years), mean (range)	62.1 (40–77)	63.2 (56–69)	67.0 (63–72)
PSA(ng/mL), mean (range)	7.3 (2.1–40)	6.4 (3.2–10.5)	9.2 (4.9–21)
D'Amico risk			
Low risk	24	0	0
Intermediate risk	44	6	5
High risk	16	9	6
Histopathology			
ISUP 1	5	0	0
ISUP 2	57	5	3
ISUP 3	15	4	5
ISUP 4	3	1	1
ISUP 5	4	5	2

prediction of seminal vesicle invasion, mp-MRI has high sensitivity and specificity (Se=0.80, Sp=0.99, PPV=0.80, and NPV=0.99). The median of the MRI-determined RD is 1.8 mm (range 1.4–4.8 mm; mean: 2.1 mm). Between the MRI-determined RD and the pathologic RD, there exist moderate correlation ($\rho=0.45, P<0.01$).

In prediction of pathologic EPE and discrimination of the high-grade EPE from the low-grade EPE, performances of the T2 WI signs, namely CBI, OEPE, NAI, and ORA, are as listed in Table 2. CBI offers high sensitivity but low specificity (Se=0.81 and Sp=0.40). OEPE, NAI, ORA features do all reveal low sensitivities (Se=0.23–0.41) but high specificities (Sp=0.83–0.97). In assessing the grade of EPE, CBI is not a beneficial MRI measure since all patients with EPE present CBI regardless of the grade of EPE. NAI shows high specificity but low sensitivity (Sp=0.93 and Se=0.45). OEPE and ORA provides perfect to high sensitivities (Se=1.00 and 0.80) with low- to medium specificities (Sp=0.30 and 0.67).

Tables 3 shows the six univariate logistic regression models developed to detect pathologic EPE. First two models employ the clinical parameters D’Amico risk stratification (DRS) or the prostate-specific antigen (PSA). Each of the remaining four models uses a single MRI-determined measure. In all models, the MRI measures and the clinical parameters are significant predictors ($P<0.05$), however, all the models suffer from poor detection performances (AUC=0.46–0.61). Multivariate logistic regression models developed to detect EPE using the clinical parameters, the MRI measures, and the combination of the clinical parameters and the MRI measures are as seen in Table 4. The models perform better than the univariate models and

achieve fair to good performances (AUC=0.69–0.84). The model that employs both the clinical parameters and the MRI measures accomplish the highest performance among the models (AUC=0.84, 95% CI 0.76–0.92).

Table 5 lists the six univariate logistic regression models developed to distinguish low-grade EPE from high-grade EPE. In these models, both the MRI-determined measures and the clinical parameters possess varying significance levels ($P=0.048–0.670$). The models using the MRI measures show poor to fair performances (AUC=0.60–0.72). The model employing the clinical parameter DRS fails (AUC=0.55), but the other model employing the clinical parameter PSA, offers a fair performance (AUC=0.73, 95% CI 0.53–0.94) which is the best one among the performances revealed by all the models developed to detect the grade of EPE. Multivariate logistic regression models developed to predict the EPE grade based on the clinical parameters, the MRI-determined measures, and the combination of the parameters and the measures are seen in Table 6. In these models, both the MRI measures and the clinical parameters retains varying significance levels ($P=0.058–0.693$). Multivariate models perform better than the univariate models by offering fair to good performances (AUC=0.72–0.85). The model that employs both the clinical parameters and the MRI-determined measures offers the best performance (AUC=0.85, 95% CI 0.70–0.99). Overall, logistic regression models incorporating clinical parameters and MRI-determined measures provide higher performances than the models employing clinical parameters or MRI-determined measures alone.

Table 2 Performances of the MRI-determined measures

	In predicting EPE				In assessing the EPE grade			
	Se	Sp	PPV	NPV	Se	Sp	PPV	NPV
CBI	0.81	0.40	0.30	0.87	–	–	–	–
OEPE	0.23	0.97	0.75	0.80	1.00	0.30	0.48	1.00
NAI	0.41	0.83	0.41	0.83	0.45	0.93	0.83	0.70
ORA	0.27	0.91	0.47	0.80	0.80	0.67	0.36	0.93

Table 3 Univariate logistic regression models to predict EPE

Origin	Parameter	B	OR	CI for OR	P-value	AUC	CI for AUC
Clinic	PSA	–1.41	0.24	0.14, 0.42	<0.001	0.50	0.37, 0.63
Clinic	DSR _{Low}	Ref.	–	–	–	0.46	0.35, 0.57
	DSR _{Intermediate}	–1.39	0.25	0.13, 0.48	<0.001		
	DSR _{High}	–0.19	0.82	0.41, 1.67	0.591		
MRI	CBI	–0.93	0.39	0.24, 0.64	<0.001	0.61	0.49, 0.73
MRI	ORA	–1.39	0.25	0.15, 0.41	<0.001	0.57	0.43, 0.70
MRI	NAI	–1.53	0.22	0.12, 0.38	<0.001	0.61	0.47, 0.74
MRI	OEPE	–1.46	0.23	0.14, 0.38	<0.001	0.60	0.47, 0.74

Table 4 Multivariate logistic regression models to predict EPE

Origin	Parameters	<i>B</i>	OR	CI for OR	<i>P</i> -value	AUC	CI for AUC
Clinic	PSA	-2.94	0.05	0.01, 0.23	<0.001	0.77	0.68, 0.86
	DSR _{Low}	Ref.	-	-	-		
	DSR _{Intermediate}	0.87	2.39	0.65, 8.75	0.189		
	DSR _{High}	2.52	12.37	2.79, 54.8	0.001		
MRI	CBI	-1.20	0.30	0.08, 1.15	0.080	0.69	0.57, 0.80
	ORA	1.15	3.16	0.34, 29.4	0.312		
	NAI	-0.15	0.86	0.22, 3.29	0.823		
	OEPE	-2.06	0.13	0.01, 1.12	0.063		
Clinic and MRI	PSA	-1.97	0.14	0.01, 1.38	0.092	0.84	0.76, 0.92
	DSR _{Low}	Ref.	-	-	-		
	DSR _{Intermediate}	2.44	11.4	1.12, 117	0.040		
	DSR _{High}	4.21	67.6	5.15, 888	0.001		
	CBI	-0.84	0.43	0.10, 1.87	0.261		
	ORA	1.45	4.24	0.35, 51.8	0.257		
	NAI	0.17	1.18	0.24, 5.69	0.836		
	OEPE	-4.03	0.02	0.00, 0.27	0.004		

Table 5 Univariate logistic regression models to assess the EPE grade

Origin	Parameter	<i>B</i>	OR	CI for OR	<i>P</i> -value	AUC	CI for AUC
Clinic	PSA	-0.23	0.90	0.32, 1.99	0.624	0.73	0.53, 0.94
Clinic	DSR _{Low}	Ref.	-	-	-		
	DSR _{High}	-0.59	0.56	0.19, 1.66	0.292	0.55	
MRI	CBI	-0.18	0.83	0.36, 1.93	0.670	0.60	0.38, 0.82
MRI	ORA	-1.03	0.36	0.13, 0.99	0.048	0.72	0.50, 0.94
MRI	NAI	-1.01	0.36	0.12, 1.14	0.083	0.67	0.44, 0.89
MRI	OEPE	-1.03	0.36	0.13, 0.99	0.048	0.72	0.50, 0.94

Table 6 Multivariate logistic regression models to assess the EPE grade

Origin	Parameters	<i>B</i>	OR	CI for OR	<i>P</i> -value	AUC	CI for AUC
Clinic	PSA	0.44	1.55	0.34, 7.03	0.567	0.72	0.53, 0.92
	DSR _{Intermediate}	Ref.	-	-	-		
	DSR _{High}	-0.99	0.37	0.06, 2.16	0.271		
MRI	ORA	-0.64	0.53	0.02, 12.54	0.693	0.81	0.64, 0.98
	NAI	0.81	2.24	0.15, 34.0	0.561		
	OEPE	-0.64	0.53	0.02, 12.5	0.693		
	PSA	3.86	47.5	0.88, 2571	0.058		
	DSR _{Intermediate}	Ref.	-	-	-		
	DSR _{High}	-1.76	0.17	0.01, 2.21	0.177		
	ORA	-2.57	0.08	0.00, 3.22	0.178		
	NAI	0.68	1.98	0.09, 43.3	0.663		
OEPE	-0.89	0.41	0.01, 14.8	0.627			

Discussion

In predicting pathologic EPE of the prostate lesions, the role of MRI and MRI-determined measures have been studied recently [19]. MR imaging has limited

applicability in indirect detection of pathologic EPE of the prostate lesions due to its low sensitivity in local staging of the prostate cancer though it is quite valuable in assessing the invasion depth of lesions in many aggressive abdominal cancers. A recent meta-analysis shows that the sensitivity and the specificity of pooled data are,

respectively, 0.61 and 0.88 [16]. A similar performance is achieved in the current study by the 5-point Likert scale of EPE assessed by using the modified PI-RADS criteria of ESUR that leads a sensitivity and specificity pair of 0.52 and 0.90. In prediction of pathologic EPE, the MRI-determined measures EPE, OEPE, NAI, and ORA offer poor sensitivity but CBI provides better sensitivity [20]. The results of the current study are in accordance with these findings.

To the best of our knowledge, there has been no published study on measuring RD of EPE with prostate MRI and assessing the grade of EPE using T2 WI signs. The current study shows that a moderate correlation is present between the MRI-determined RD and the pathologic RD, while MRI-determined RD is usually higher than the pathologic RD. MRI visible EPE should be identified to measure the RD; however, presence of MRI visible EPE might be a late finding that indicates an advanced disease. Furthermore, measurement of the RD may be very difficult even in the presence of easily identifiable MRI visible EPE since the prostate gland has no real prostate capsule. On the other hand, MRI may overestimate the pathological RD in the presence of periprostatic venous plexus and neurovascular bundle at the posterolateral portion of the gland [21]. It seems prostate MRI is able to measure the pathologic RD only with a limited accuracy. In prediction of the EPE grade, the assessment of the T2 WI signs which linked with EPE diagnosis might provide better results.

The T2 WI signs studied show slightly different performances in assessing the EPE grade, OEPE, and ORA provide fair accuracies with high sensitivities despite their poor specificities. NAI shows fair diagnostic accuracy with poor sensitivity and high specificity and CBI delivers poor diagnostic accuracy. For all the lesions with EPE, CBI is present regardless of the risk of EPE and therefore thought to be an early indicator of EPE. The good performances of T2 WI signs of OEPE and ORA in assessing the EPE grade imply that these measures may be late indicators for EPE. The current study is in accordance with a previous study that suggested, while ‘CBI’ was an earlier indicator of EPE, ‘OEPE’ and ‘ORA’ were relatively late indicators [22]. Besides, none of these features alone achieves good performance in predicting the EPE grade. But remarkably better performances are achievable when all the MRI features are evaluated jointly with the clinical parameters using logistic regression modeling.

The median value of pathologic RD calculated for use as an optimal cut-off in distinguishing the low-grade EPE from the high-grade EPE is 1.0 mm for the current study, while reported values range from 0.6 to 2.4 mm. The median pathological RD of the current study is in accordance with several previous studies, one of which had the largest study cohort of EPE positive patients. In this previous study, it was

also reported that utilization of the median value (1 mm) as the optimal cut-off was significantly associated with the increase in BCR risk [8, 23]. Hence, the cut-off value of 1 mm was taken for sub-classifying the patients. Unfortunately, there is no common consensus in the most optimal cut-off value of pathological RD. As pathological criterion for sub-classifying patients with EPE improve, more precise radiological parameters may be achieved.

There are some limitations of the current study. Firstly, there is a possible selection bias due to its retrospective design. Secondly, T design of the current study considers only the patients who underwent surgery. This might bring some bias to the radiologists during their evaluations and some additional work on patients from a control group might minimize the bias. Thirdly, sample size of patients with EPE is relatively small for performing subgroup analysis. Finally, use of median pathologic radial distance as the optimal cut-off value to determine low-grade and high-grade EPE is questionable. Prospective multi-center study on a larger study population is needed to clarify these issues.

In conclusion, prostate MRI holds a potential not only in detecting EPE but also in predicting the grade of EPE in prostate cancer. In discrimination of high-grade and low-grade EPE, it would be very beneficial to assess T2 WI by the radiologist for the MRI features namely OEPE, ORA, and NAI that linked with EPE diagnosis. It seems that if these T2 WI signs are seen together, the probability of high-grade EPE increases. Although MRI-determined measures may provide better performances than the clinical parameters, improved performances are obtained when the clinical parameters and the MRI-determined measures are evaluated jointly in predicting the degree of EPE. Further prospective studies with a larger patient population and with multi-center data from different MRI setups are needed to figure out the potential benefits and further improvements that can be achieved by using prostate MRI in non-invasive prediction of the EPE grade in prostate cancer.

Acknowledgements We thank Tugrul Bahtiyar Koroglu, radiology technician for assistance with reviewing all the radiology databases of our institution that gave great contribution to this manuscript.

Funding This research did not receive any specific grant from funding agencies in the public, commercial, or not for-profit sectors.

References

1. Fleming ID, Cooper JS, Henson DE et al. AJCC cancer staging manual, 5th edn. Philadelphia: Lippincott-Raven, 1997.
2. Ohori M, Wheeler TM, Kattan MW, Goto Y, Scardino PT. Prognostic significance of positive surgical margins in radical prostatectomy specimens. *J. Urol.* 1995; 154: 1818–1824.
3. Epstein JI, Carmichael MJ, Pizov G, Walsh PC. Influence of capsular penetration on progression following radical prostatectomy:

- a study of 196 cases with long-term follow-up. *J. Urol.* 1993; 150: 135–141.
4. Wheeler TM, Dillioglulil O, Kattan MW et al. Clinical and pathological significance of the level and extent of capsular invasion in clinical stage T1–2 prostate cancer. *Hum. Pathol.* 1998; 29: 856–862
 5. Davis BJ, Pisansky TM, Wilson TM, Rothenberg HJ, Pacelli A, Hillman DW, Sargent DJ, Bostwick DG. The radial distance of extraprostatic extension of prostate carcinoma: implications for prostate brachytherapy. *Cancer.* 1999;85(12):2630–7.
 6. Sung MT, Lin H, Koch MO, Davidson DD, Cheng L. Radial distance of extraprostatic extension measured by ocular micrometer is an independent predictor of prostate-specific antigen recurrence: a new proposal for the substaging of pT3a prostate cancer. *Am. J. Surg. Pathol.* 2007; 31: 311–318.
 7. van Veggel BA1, van Oort IM, Witjes JA, Kiemeny LA, Hulsbergen-van de Kaa CA. Quantification of extraprostatic extension in prostate cancer: different parameters correlated to biochemical recurrence after radical prostatectomy. *Urology.* 2000;55(3):382–6.
 8. Danneman D, Wiklund F, Wiklund NP, Egevad L. Prognostic significance of histopathological features of extraprostatic extension of prostate cancer. *Histopathology.* 2013;63(4):580–9. doi: 10.1111/his.12199. Epub 2013 Jul 26.
 9. Edge SB, Byrd DR, Compton CC, Pritz AG, Greene FL, Trotti A. *AJCC cancer staging manual*. 7th edn. New York: Springer, 2010.
 10. Barentsz JO, Richenberg J, Clements R, et al. ESUR prostate MR guidelines 2012. *EurRadiol* 2012;22:746–757
 11. Eberhardt SC, Carter S, Casalino DD, et al. ACR Appropriateness Criteria prostate cancer—pretreatment detection, staging, and surveillance. *J Am CollRadiol* 2013;10:83–92.
 12. Weinreb JC, Barentsz JO, Choyke PL, Cornud F, Haider MA, Macura KJ, Margolis D, Schnall MD, Shtern F, Tempny CM, Thoeny HC, Verma S. PI-RADS Prostate Imaging Reporting and Data System: 2015, Version 2. *Eur Urol.* 2016;69(1):16–40.
 13. Morlacco A, Sharma V, Viers BR, et al. The incremental role of magnetic resonance imaging for prostate cancer staging before radical prostatectomy. *Eur Urol* 2017;71(5):701–704.
 14. Feng TS, Sharif-Afshar AR, Wu J, et al. Multiparametric MRI improves accuracy of clinical nomograms for predicting extracapsular extension of prostate cancer. *Urology* 2015;86(2):332–337.
 15. Schieda N, Quon JS, Lim C, El-Khodary M, Shabana W, Singh V, Morash C, Breau RH, McInnes MD, Flood TA. Evaluation of the European Society of Urogenital Radiology (ESUR) PI-RADS scoring system for assessment of extra-prostatic extension in prostatic carcinoma. *Eur J Radiol.* 2015;84(10):1843–8.
 16. de Rooij M, Hamoen EH, Witjes JA, Barentsz JO, Rovers MM. Accuracy of magnetic resonance imaging for local staging of prostate cancer: a diagnostic meta-analysis. *Eur Urol* 2016; 70:233–24.
 17. Krishna S, Lim CS, McInnes MDF, et al. Evaluation of MRI for diagnosis of extra-prostatic extension in prostate cancer. *J Magn Reson Imaging* 2018;47(1):176–185.
 18. Sung MT, Lin H, Koch MO, Davidson DD, Cheng L. Re: Radial Distance of Extraprostatic Extension Measured by Ocular Micrometer is an Independent Predictor of Prostate-Specific Antigen Recurrence. A New Proposal for the Substaging of pT3a Prostate Cancer. *Am J Surg Pathol* 2007;31:311–8.
 19. Yu KK, Hricak H, Alagappan R, Chernoff DM, Bacchetti P, Zaloudek CJ. Detection of extracapsular extension of prostate carcinoma with endorectal and phased-array coil MR imaging: multivariate feature analysis. *Radiology* 1997;202(3):697–702.
 20. Mehralivand S, Shih JH, Harmon S, Smith C, Bloom J, Czarniecki M, Gold S, Hale G, Rayn K, Merino MJ, Wood BJ, Pinto PA, Choyke PL, Turkbey B. A Grading System for the Assessment of Risk of Extraprostatic Extension of Prostate Cancer at Multiparametric MRI. *Radiology.* 2019;290(3):709–719.
 21. Panebianco V, Barchetti F, Barentsz J, Ciardi A, Cornud F, Futterer J, Villeirs G. Pitfalls in Interpreting mp-MRI of the Prostate: A Pictorial Review with Pathologic Correlation. *Insights Imaging.* 2015;6(6):611–30.
 22. McEvoy SH, Raeside MC, Chaim J, Ehdai B, Akin O. Preoperative Prostate MRI: A Road Map for Surgery. *AJR Am J Roentgenol.* 2018;211(2):383–39.
 23. Sohayda C, Kupelian PA, Levin HS, Klein EA. Extent of extracapsular extension in localized prostate cancer. *Urology.* 2000;55(3):382–6.

Publisher's Note Springer Nature remains neutral with regard to jurisdictional claims in published maps and institutional affiliations.